Articular Cartilage Repair After Implantation of Hyaline Cartilage Beads Engineered From Adult Dedifferentiated Chondrocytes

Cartibeads Preclinical Efficacy Study in a Large Animal Model

Halah Kutaish, MD, PhD, Philippe Matthias Tscholl, MD, Erika Cosset, PhD, Laura Bengtsson, MSc, Vincent Braunersreuther,[#] PD, PhD, Dimitrios Stafylakis, MD, Didier Hannouche, Prof., MD, Eric Gerstel, PD, MD, Karl-Heinz Krause, Prof., MD, Mathieu Assal, PD, MD, Jacques Menetrey, Prof., MD, and Vannary Tieng,* PhD
Investigation performed at the Faculty of Medicine, University of Geneva, in collaboration with Geneva University Hospitals, Geneva, Switzerland

Background: Chondrocyte-based cell therapy to repair cartilage has been used for >25 years despite current limitations. This work presents a new treatment option for cartilage lesions.

Hypothesis: High-quality hyaline cartilage microtissues called Cartibeads are capable of treating focal chondral lesions once implanted in the defect, by complete fusion of Cartibeads among themselves and their integration with the surrounding native cartilage and subchondral bone.

Study Design: Controlled laboratory study.

Methods: Cartibeads were first produced from human donors and characterized using histology (safranin O staining of glycosaminoglycan [GAG] and immunohistochemistry of collagen I and II) and GAG dosage. Cartibeads from 6 Göttingen minipigs were engineered and implanted in an autologous condition in the knee (4 or 5 lesions per knee). One group was followed up for 3 months and the other for 6 months. Feasibility and efficacy were measured using histological analysis and macroscopic and microscopic scores.

Results: Cartibeads revealed hyaline features with strong staining of GAG and collagen II. High GAG content was obtained: 24.6-μg/mg tissue (wet weight), 15.52-μg/mg tissue (dry weight), and 35 ± 3-μg GAG/bead (mean ± SD). Histological analysis of Göttingen minipigs showed good integration of Cartibeads grafts at 3 and 6 months after implantation. The Bern Score of the histological assay comparing grafted versus empty lesions was significant at 3 months (grafted, n = 10; nongrafted, n = 4; score, 3.3 and 5.3, respectively) and 6 months (grafted, n = 11; nongrafted, n = 3; score, 1.6 and 5.1).

Conclusion: We developed an innovative 3-step method allowing, for the first time, the use of fully dedifferentiated adult chondrocytes with a high number of cell passage (owing to the extensive amplification in culture). Cartibeads engineered from chondrocytes hold potential as an advanced therapy medicinal product for treating cartilage lesions with established efficacy.

Clinical Relevance: This successful preclinical study, combined with standardized manufacturing of Cartibeads according to good manufacturing practice guidelines, led to the approval of first-in-human clinical trial by the ethics committee and local medical authority. The generated data highlighted a promising therapy to treat cartilage lesions from a small amount of starting biopsy specimen. With our innovative cell amplification technology, very large lesions can be treated, and older active patients can benefit from it.

Keywords: autologous hyaline cartilage implantation; articular cartilage; dedifferentiation; hyaline cartilage tissue engineering (3D); microtissues

The American Journal of Sports Medicine
2023;51(1):237–249
DOI: 10.1177/03635465221138099

Cartilage lesions constitute an essential part of musculoskeletal health conditions, with a prevalence reaching 63% of the general population and 36% of athletes.[26,27] The goals of treatment focus on immediate symptom alleviation,

return to active life, and the durability of the treatment results, all while slowing or stopping further damage.[27] Current treatment modalities for cartilage damage range from conservative (nonoperative) to minimally invasive surgery to joint replacement or fusion.[31] To reduce pain and inflammation, nonoperative management is offered with medication and physical therapy. However, this does not address the structural deficit of the missing cartilage in the joint. Moreover, solid evidence of structural improvement with such modalities remains missing.[13]

Over the past 30 years, researchers have tried to recreate the structural and biochemical features of hyaline cartilage through tissue engineering and cell modulation.[9,21] The objective is to offer a long-lasting repair of the chondral defects. Indeed, the avascular and unenervated qualities of articular cartilage might be responsible for its poor autorepair and healing. Additionally, this makes it hard for most graft material to integrate with the native cartilage and/or the subchondral bone. If left untreated, cartilage injury can progress toward osteoarthritis.

Despite being used for >25 years, chondrocyte-based cell therapy to regenerate cartilage still has some limitations.[25,39] Chondrocytes represent a logical cell source for cartilage regeneration. Indeed, only this cell type is involved in the maintenance of the hyaline cartilage matrix, characterized by the presence of glycosaminoglycan (GAG) and type II collagen.[6,41] A major challenge is that adult chondrocytes tend to dedifferentiate into fibroblast-like cells in monolayer culture, resulting in rapid loss of function usually occurring at the second or third cell passage.[5,20] Dedifferentiated chondrocytes are characterized by the loss of production of the main constituents of hyaline cartilage (type II collagen and GAG). Instead, dedifferentiated chondrocytes produce type I collagen, present in fibrocartilage. Fibrocartilage is biomechanically different from hyaline cartilage and is not considered an effective long-lasting tissue because it leads to dysfunctional repair.[14] Fibrocartilage is also produced in the treatment by microfractures.[22,23] Another challenge for autologous chondrocyte-based cell therapy is the difficulty to expand and differentiate cells from elderly patients, limiting their use in this population. Consequently, most clinical trials limit the inclusion to patients aged <55 years.[3,4,28]

Cell-based therapies using autologous chondrocyte implantation (ACI) are still indicated for cartilage lesions >2 cm^2. Currently, only 5 ACI-based therapies have been approved for focal cartilage lesions[31,36]: matrix-induced ACI (MACI; Vericel),[10,36] Spherox (Co.don),[11,33] Chondron (Sewon Cellontech), Cartigrow (Regrow Bioscience),[34] and Ortho-ACI (Orthocell). None of these products show high-quality hyaline cartilage tissue before and after transplantation. Chondron, Cartigrow, and Otho-ACI are not tissues per se but chondrocytes in suspension combined or not with scaffold for implantation. In phase 3 studies, Spherox did not show superiority to microfracture[33] unless low-passage cells were used,[12] and Vericel acknowledges that there is no difference with microfracture based on magnetic resonance imaging data.[37]

Long-term success in the treatment of cartilage lesions requires implantation and integration of high-quality hyaline transplant resembling native cartilage.[25,31] In this work, we describe an innovative method allowing extensive culture of adult dedifferentiated human chondrocytes, from donors >80 years old, used to generate cartilage microtissues (Cartibeads). Cartibeads produce their own hyaline extracellular matrix without the support of an external scaffold, with biochemical composition close to that of native articular cartilage.

We hypothesize that Cartibeads are capable of treating focal chondral lesions once implanted in the defect by complete fusion of Cartibeads among themselves and their integration with the surrounding native cartilage and subchondral bone. Moreover, given their size (diameter, 1.5-2 mm), Cartibeads can be grafted by minimally invasive surgery or arthroscopy with a loading instrument adapted to graft implantation (Chondrectom Kit; biovico.pl).

METHODS

Production of Cartibeads

Human cartilage samples were obtained from consenting living donors (age, 18-80 years) after orthopaedic procedures for various indications. The collected cartilage was transferred to the laboratory in a sterile recipient in normal saline (NaCl 0.9%) at room temperature. Minipig cartilage samples were obtained during the harvest surgery described here.

The cartilage (human or minipig) was sliced into small pieces (1 mm) to facilitate the extraction of chondrocytes by enzymatic digestion and then placed in rotation at 37°C overnight with collagenase type II (400 U/mL; Thermo Fisher). Once extracted, chondrocytes were cultured in 2-dimensional (2D) monolayer culture (Figure 1). All 2D cell cultures were conducted on extracellular matrix–coated flasks (T25 cm^2) and in atmospheric oxygen conditions (21%) with 10% CO_2. At confluence, cells were passaged in 1 T75-cm^2 flask (passage 1) and split later

*Address correspondence to Vannary Tieng, PhD, Vanarix SA, Avenue Mon-Repos 14, Lausanne, 1005, Switzerland (email: Vannary.tieng@vanarix-sa.ch).

All authors are listed in the Authors section at the end of this article.

H.K. and P.M.T. contributed equally to this article.

Submitted March 22, 2022; accepted September 9, 2022.

One or more of the authors has declared the following potential conflict of interest or source of funding: This work was supported by Vanarix SA. V.T. has received commercial research support from Vanarix, is the CEO of Vanarix, and holds the patent for Cartibeads. H.K. has received research support from Vanarix SA. L.B. has received commercial research support from Vanarix SA and is employed by Vanarix SA. AOSSM checks author disclosures against the Open Payments Database (OPD). AOSSM has not conducted an independent investigation on the OPD and disclaims any liability or responsibility relating thereto.

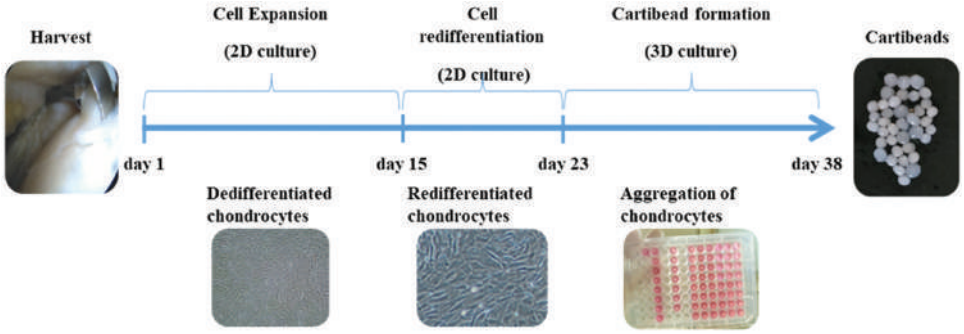

Figure 1. Production scheme of Cartibeads in 2- and 3-dimensional culture.

into 2 T75-cm^2 flasks (passage 2) to reach confluence. Cells were expanded for 12 to 16 days in expansion medium (Dulbecco's modified Eagle medium [DMEM] with high glucose; Gibco), 10% human serum (Sigma), 1× L-glutamine, 1× penicillin-streptomycin (10378016; Thermo Fisher), 1× nonessential amino acids (Gibco), 20-ng/mL FGF2, 10-ng/mL PDGF-BB, and 5-ng/mL TGF-β3 (Cell Guidance).

After extensive expansion, chondrocytes were redifferentiated for 7 days in redifferentiation medium (DMEM with high glucose; Gibco), 10% human platelet lysate containing a high concentration of PDGF (PDGF-BB, ~9 ng/mL; PDGF-AB, ~35 ng/mL) and TGF-β1 (~140 ng/mL) and a low concentration of FGF2 (<0.05 ng/mL; Sexton Biotech), 1× L-glutamine, 1× penicillin-streptomycin (10378016; Thermo Fisher), and 1× nonessential amino acid (Gibco). Chondrocytes used to generate Cartibeads were cultured at passages 5 to 9.

In the 3-dimensional step, chondrocytes were collected and aggregated in chondrogenic medium (DMEM with high glucose), 1× ITS-X, 1× L-glutamine, 1× penicillin-streptomycin (10378016; Thermo Fisher), 1× nonessential amino acid (11140050; Gibco), ascorbic acid (200 μM; Sigma), 40-ng/mL TGFβ3, 40-ng/mL BMP2, and 40-ng/mL IGF (Cell Guidance) to obtain 0.2 × 10^6 cells/well (1 Cartibeads per well) in conical 96-well polypropylene plates (~20 × 10^6 cells/plate). The 96-well plates were centrifugated 5 minutes at 300*g* to allow cell aggregation and formation of Cartibeads after 15 days in 3-dimensional culture (Figure 1).

The standard protocol method uses the same protocol, mediums, culture conditions, and reagents of the Cartibeads method except for step 2 (cell redifferentiation in 2D). In the standard protocol method, the expanded dedifferentiated chondrocytes directly undergo the bead formation by aggregation in 96-well plates without being redifferentiated.

GAG Quantification

GAG content was evaluated by the dimethylmethylene blue assay (341088; Sigma). Chondroitin sulphate A (C9819; Sigma) was used to generate 6 standards, with concentrations ranging from 0 to 50 μg/mL. Chondroitin sulphate C (C4384; Sigma) was used to generate a low and high internal quality control: concentrations of 15 and 35 μg/mL, respectively. Cartibeads were digested with proteinase K (1 mg/mL, V3021; Promega) in Tris-HCl, 50 mM, and pH 8 (Sigma) for 15 ± 2 hours at 56°C. The enzymatic digestion was stopped by incubation at 97°C for 15 minutes. The resulting sample was diluted (1:5-1:10) in Tris-HCl, 50 mM, and pH 8 for the assay. Finally, 100 μL of standards, internal quality controls, and samples were read with a spectrophotometer in triplicates (λ = 525 nm) after 5-minute reaction with 1-mL dimethylmethylene blue assay solution.

Immunohistochemical Staining

For immunohistochemical staining of formalin-fixed paraffin-embedded cartilage tissues and Cartibeads, the paraffin blocks containing the samples were cut with the microtome at 5 μm. The slides were dried overnight at 47°C. Slides were deparaffinated by xylol and rehydrated by consecutive alcohol baths (concentrations, 100%, 95%, and 70%). Two techniques of unmasking were used. For native cartilage coming from minipigs, we used a 20-mg/mL solution of hyaluronidase in 0.1M phosphate buffer, placed on slides for 1 hour at 37°C. Slides were rinsed in phosphate-buffered saline (PBS) twice for 5 minutes to remove hyaluronidase. Cartibeads samples were immersed in a 0.01M citrate buffer bath at pH 6, heated 3 times, 5 minutes each in a microwave at 620 W, and cooled in an ice bath for 20 minutes. The slides were then rinsed in PBS for 5 minutes. The primary antibodies were then used: collagen I (ab34710; Abcam), collagen II (ab34712 [Abcam]; SAB4500366 [Sigma]), and collagen X (ab49945; Abcam). Of note, the 2 type II collagen antibodies showed similar results. The antibodies were placed on different samples and diluted 1:100 in 0.3% Triton X-100 in PBS for 1 hour. After rinsing for 5 minutes with PBS, secondary antibodies were used: a biotin-conjugated anti-mouse IgG (BA-2000; Vector Labs) and anti-rabbit IgG (BA-1000; Vector Labs) and an avidin-biotin-peroxidase detection system with 3,3′-diaminobenzidine substrates (Vector Labs). Samples were counterstained with pure-filtered hematoxylin. Dehydration was achieved by vigorous shaking of the rack 10 to 20 times in alcohol baths (concentration, 95% and 100%), followed by a pure xylol bath until slide assembly with Eukitt resin (batch A1113, KiNDO1500, Orsatec). A

Nikon Eclipse C1 confocal microscope and a Nikon Eclipse TE2000-E were used for imaging.

Safranin O Staining

Safranin O staining of cartilage spheres and native cartilage formalin-fixed paraffin-embedded samples was performed to reveal GAGs on 5-μm paraffin slices. Slides were deparaffinated by xylol and rehydrated by consecutive alcohol bath (concentration, 100%, 95%, and 70%) with a final 5-minute distilled water bath. Then, hematoxylin staining was used for nucleus counterstaining, followed by a 5-minute wash with running hot water. Fast Green (Sigma F7252) was used to stain the cytoplasm and then washed out with acetic acid. The slides were washed out immediately with distilled water. Safranin O 0.1% in water bath (Sigma S2255) was applied for staining of GAGs for 2.5 minutes and then washed repeatedly with distilled water. Dehydration was achieved by vigorous shaking of the rack 10 to 20 times in alcohol baths (concentration, 95% and 100%), followed by a xylol bath until slide assembly with Eukitt resin (Batch A1113, KiNDO1500).

Cell Viability of Cartibeads

Cartibeads samples were tested for viability using the red fluorescent dye Zombie Aqua (423101; Biolegend), which is an amine-reactive fluorescent dye that is nonpermeant to living cells but permeant to cells with compromised membranes, thus allowing assessment of live versus dead cells. Three-dimensional samples were collected by the end of step 3 and washed with PBS; then, Zombie dye diluted in PBS (1:100) was added for 20 minutes. Samples were kept in the dark for 1 hour. Samples were subsequently cut with a cryostat microtome at 3 μm of thickness and mounted on Superfrost Plus slides. Afterward, they were fixed with formaldehyde 4% and treated with Hoechst (Molecular Probe H3570; Thermo Fisher) diluted in PBS (1:2000) for 10 minutes. Positive control for the assay was achieved using Triton 10% (X100-100ML; Sigma) in PBS for 1 hour at room temperature before the Zombie dye step.

Biomechanical Measurements

Compression tests were performed with an MTS criterion pull-push machine (model 42) equipped with a 1-N load cell on cartilage beads ranging from 0.68 to 1.54 mm in diameter and in native cartilage. Compression speed was set at 0.01 $m \cdot s^{-1}$ with a maximum load compression imposed at 0.2 N to stay/keep as much as possible in the linear regime of the cartilage; a maximum 20 beads were used per test to increase the probed surface area. An original holding system was custom-made to avoid sliding of the beads and ensure an isotropic confined compression during the test, which does not perfectly represent the in vivo situation. To put the beads at the bottom of the chamber and to increase the contact surface with the piston, a first test per sample without measurement was performed. Compression force as a function of displacement was measured as raw data (once per sample). The stress-strain curve was then calculated to estimate the Young modulus of the cartilage, considering the slope of the data set in the linear regime, divided by the surface area of the sample and the number of the beads for normalization purposes. The calculation of the Young modulus was made as follows: $E = \sigma/\epsilon$, where σ is the compression stress (kilopascal), E is the Young modulus (kilopascal), and ϵ is the strain (no unit) corresponding to the normalized elongation.

Hematoxylin and Eosin Staining

Hematoxylin and eosin staining was performed with the HE600 de Ventana (Roche).

Implantation of Autologous Cartibeads in Minipig for Efficacy Study

Animal procedures were approved by the Swiss Federal Veterinary Office (GE/60/18).

Göttingen minipigs were chosen for their cartilage maturity and for knee anatomy resembling that of humans.[16] Six adult female minipigs aged 19 to 22 months (37-48 kg) were used in the study with a planned 5 lesions per knee (planned, n = 30; achieved, n = 28). The animals were anesthetized with sevoflurane and given a prophylactic antibiotic intravenously (cefazolin, 2 g/kg) 30 minutes before the incision. They were operated under complete narcosis and extubated 5 minutes after skin closure. Skin disinfection was repeated 3 times, and aseptic draping was performed with dischargeable surgery drapes.

Harvest Surgery. Minipig cartilage samples (~30 mg) were obtained from the lateral trochlear, harvested from the right knees of the minipigs. A supralateral parapatellar approach was chosen for the first operation. Cartilage harvesting was performed at the superolateral border of the lateral trochlear facet to prevent potential conflict with later cartilage lesions during the second surgical step. The cartilage biopsy specimens were put into expansion medium for processing. A stepwise closure was performed. No bandage was applied.

Minipig Cartibeads were produced as described in the Methods section.

Cartibeads Implantation Surgery. Five to 6 weeks after cartilage harvesting, the minipigs underwent the second operation through a medial parapatellar tendon approach. By this approach, 2 lesions on the medial and lateral femoral trochlea each were created in all minipigs except 1, owing to extent of the donor site. Full chondral lesions were made each time, so the thickness varied among minipigs ($\leq$1 mm). Lesions 6 mm in diameter were created by a small curette and then filled completely by a single layer of 4 or 5 Cartibeads. For faster attachment, a thin layer of Tisseel (Baxter) was added to each defect after the deposition of the Cartibeads. A fifth lesion was created on the medial femoral condyle, on a weightbearing zone, and filled with

Cartibeads in identical manner. In each animal, 1 lesion was kept empty at a different location as a negative control. A stepwise closure was performed. No bandage was applied.

Efficacy was based on the number of lesions (grafted, n = 21; nongrafted, n = 7).

Rehabilitation. Full weightbearing was allowed as soon as the narcosis was finished, with no restriction of any activity.

Euthanasia. Three minipigs (Nos. 4-6) were sacrificed 3 months after the second operation, and the other 3 minipigs (Nos. 1-3) were sacrificed at 6 months.

Joint Processing for Histology. The operated knee was amputated, and the distal femur was put in formyl aldehyde solution for 2 days for histological analysis. Each biopsy specimen containing the holes to be analyzed was recut in the joint before being completely decalcified in EDTA solution, dehydrated in alcohol solutions of increasing concentration, and then cleared in xylene before embedding in paraffin. The embedded sites were then longitudinally cut in the middle of the implantation site (5-μm thickness) using a microtome. For each site, sections were performed and proceeded to safranin O staining, hematoxylin and eosin, or immunohistochemistry analysis.

Scoring

Macroscopic and microscopic scores were graded by 2 independent blinded examiners with the results reviewed by a third person to calculate the score and perform the statistical analysis.

Macroscopic Scoring: Goebel Reverse Score. The Goebel Reverse Score[15] consists of 5 major parameters (color of repair tissue, presence of blood vessels in repair tissue, surface of repair tissue, filling of the defect, degeneration of the adjacent articular cartilage) and 25 items (5 items for each major parameter with 0-4 points: 0 = best/excellent cartilage, 4 = worst/empty lesion). A total number of 20 points is achieved for the worst possible result.

Microscopic Scoring: Bern Score. The Bern Score[17] accounts for uniformity and intensity of matrix staining, cell density/extent of matrix produced, and cellular morphologies.

Quantification and Statistical Analysis

Sample size and statistics for each experiment are provided in the Results section and/or figure legends. One-way analysis of variance was used for the statistical analyses (except when Student *t* test was indicated), with $P < .05$ considered significant.

Availability of Data and Materials

The composition of the Cartibeads cell culture mediums described in the Methods are under patent WO2021028335. Moreover, raw data will be available upon request.

RESULTS

Human Cartibeads Characterization

Cartibeads from human donors were generated according to a standardized protocol as described in the Methods section. Different readouts were measured to characterize the Cartibeads. Histological qualitative analyses of human Cartibeads showed the presence of hyaline features with a homogeneous distribution of safranin O–stained GAG and strong immunodetection of type II collagen, whereas type I collagen staining was faint (Figure 2). We were able to engineer Cartibeads of high hyaline quality from adult dedifferentiated chondrocytes cultured from donors up to 80 years of age, including chondrocytes from patients with osteoarthritis (see Appendix Table A1, available in the online version of this article).

Quantitative analysis of Cartibeads revealed high GAG content: 24.6-μg/mg tissue (wet weight) and 15.52-μg/mg tissue (dry weight), which was independent of patient age and osteoarthritic status of the joint (Figure 3A; Appendix Table A1, available online). When compared with the beads obtained by a standard culture protocol, Cartibeads showed a significantly improved GAG content, quantitatively and qualitatively (Figure 3B). Indeed, Cartibeads showed 35 ± 3–μg GAG/bead (mean ± SD).

In cell therapy, the viability assessment of cellular components of the transplanted material is essential. Thus, we evaluated the proportion of viable cells within Cartibeads in different conditions. Viability of the cells inside Cartibeads was determined at the end of the culture cycle, and a slight number of dead cells (2% at 20°C and 13% at 4°C) were detected at day 6, suggesting good survival of the chondrocytes in the Cartibeads (Appendix Figure A1a, available online). To characterize the biomechanical properties of Cartibeads, we calculated the Young modulus.[24] The values obtained from 6 donors are in the range of 60 to 358 Pa per Cartibead, which is very low in comparison with native cartilage (~25 kPa) (Appendix Figure A1b). These values were expected as Cartibeads are immature neocartilage tissues.

Preclinical Efficacy Study In Vivo

To move toward clinical application, we performed a preclinical efficacy study in adult Göttingen minipigs. The study interventions are detailed in the Methods section. Briefly, we performed a first operation to harvest minipig cartilage and then a second to create 4 or 5 lesions per animal/right knee and to implant autologous Cartibeads (Appendix Figure A2, a and c, available online). Before implantation, the amount of GAG in the minipig Cartibeads was quantified and ranged between 40 and 50 μg/bead on average (Appendix Figure A2b). Moreover, we characterized minipig Cartibeads histologically. Staining with safranin O showed the presence of GAG (Appendix Figure A2d), with strong immunodetection of collagen II, weak staining for collagen I, and the absence of staining for collagen X (Appendix Figure A2e).

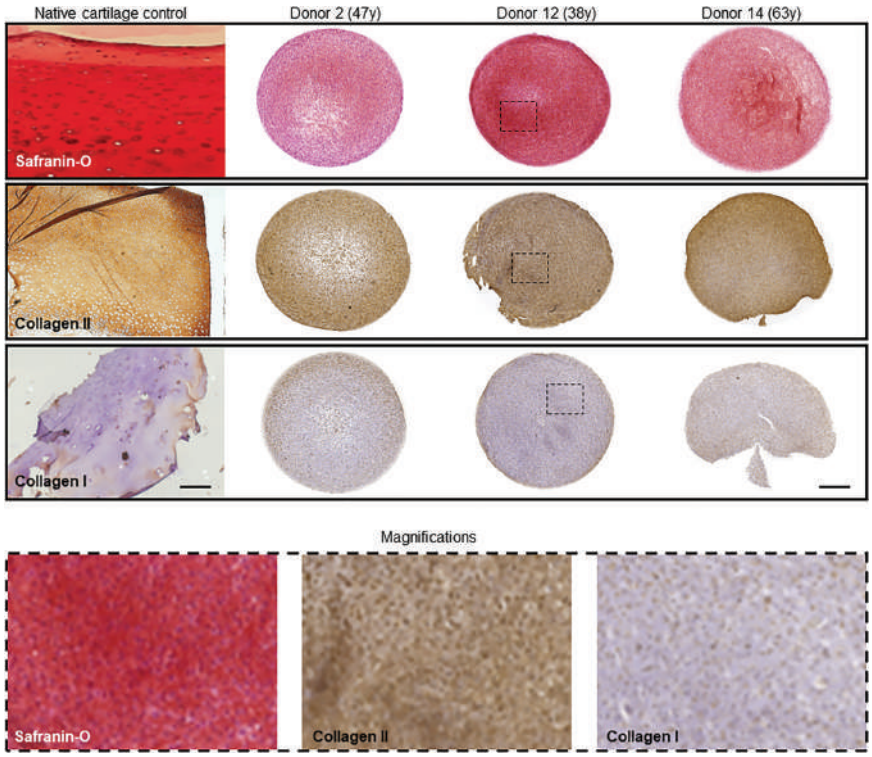

Figure 2. Histological analysis of human Cartibeads from fixed samples. Representative images of safranin O staining of glycosaminoglycan (GAG; red, top panel) and strong immunodetection of type II collagen (DAB staining, middle panel), characterizing hyaline cartilage, and weak type I collagen detection (lower panel) of Cartibeads obtained from 3 independent donors. Chondrocytes were used at passage 5 to form Cartibeads. Scale bar: 200 and 500 μm for the Cartibeads and native cartilage, respectively. Magnification of stained Cartibeads is provided for better assessment of cellular structure (dotted panel).

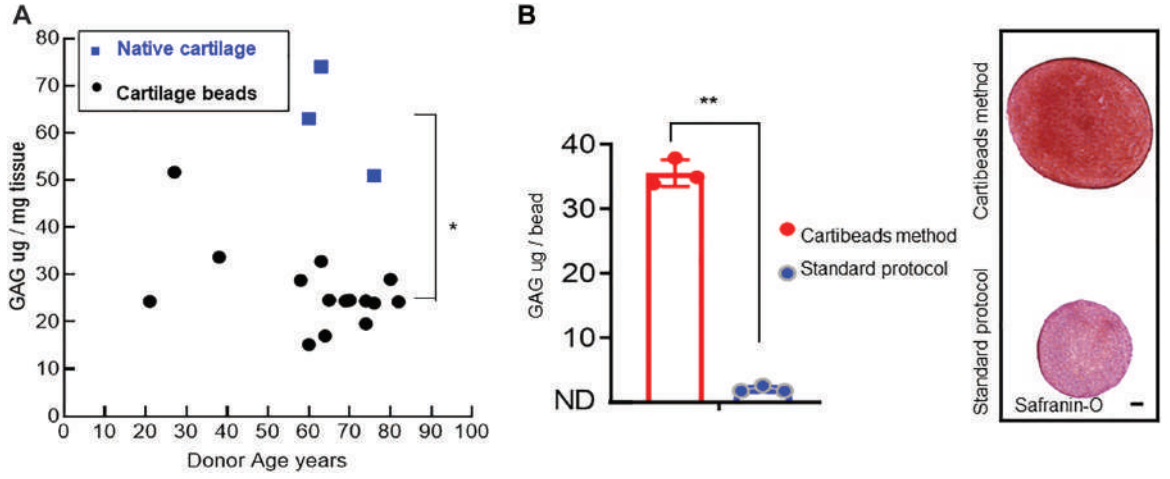

Figure 3. Cartibeads glycosaminoglycan (GAG) content. (A) Biochemical quantification of GAG content in Cartibeads (μg/mg tissue, wet weight) was determined with dimethylmethylene blue assay from 15 donors (black dots) and 3 native cartilage controls (blue square). (B) GAG content of Cartibeads versus beads obtained by standard protocol shown quantitatively (GAG μg/bead) and qualitatively (safranin O staining). Chondrocytes were used between passages 5 and 9. Values are presented as mean ± SD. *$P < .05$. **$P < .001$. Scale bar: 100 μm.

The minipigs were followed for either 3 months (Figure 4) or 6 months (Figure 5). At 3 months after implantation, we assessed the hyaline features of the created minipig lesions by safranin O staining. A complete fusion of Cartibeads and their integration within the surrounding native cartilage and subchondral bone were observed in the grafted lesions. We also observed the presence of fibrohyaline cartilage in grafted lesions (Figure 4A, top panels) and mainly fibrocartilage in the control lesions (Figure 4A, bottom panels). The graft maintained hyaline quality as shown by the intense detection of GAG by safranin O staining and the detection of collagen II associated with a weak detection of collagen I and X (Figure 4, B through D).

Similar results were observed in the lesions at 6 months after implantation (Figure 5, A through D). The lesions left untreated showed the presence of fibrocartilage with intense detection of collagen I and weak or absent collagen II staining (Figures 4B and 5B). Although we did not reach significance for the Goebel Reverse Score, we found a trend toward a significant difference (Figures 4E and 5E). However, we noted a significant difference in the quality of the repaired tissue according to the Bern Score (Figures 4F and 5F).

Additionally, the histological analyses revealed cartilage regeneration using the Cartibeads treatment. Indeed, Cartibeads produced mature tissue characterized by an organization in 3 layers, similar to that of native cartilage: a surface zone with elongated cells, middle and deep zones with mature round-shaped chondrocytes within lacuna, and a columnar organization adjacent to the subchondral bone (Figure 6A). These distinct layers were not observed in the fibrocartilage organization from the control lesion (Figure 6B). Collectively, the autologous Cartibeads proved their efficacy in terms of engraftment in the lesions while preserving their hyaline quality. They also proved to be safe, as neither degeneration of the joint nor ectopic or hypertrophic tissue formation was noted at macroscopic inspection by 2 independent observers (Appendix Figure A2c, available online).

DISCUSSION

In this work, we showed the hyaline-like features of Cartibeads and their ability to repair knee cartilage lesions in minipigs with preserved quality and good integration. To date, available cartilage regeneration techniques have produced fibrocartilage or fibrohyaline cartilage with poor/limited integrative capacities and higher friability.[8,19] This is less than optimal, as fibrocartilage does not have the same physical and biochemical properties as the native articular cartilage and is less resistant to axial and shear forces that the joint is subjected to; thus, it tends to delaminate within few years after implantation. However, MACI showed favorable results in a recently published systematic review and meta-analysis by Grossman et al.[18] The authors concluded that all subscales were improved when evaluated after 2 years and that MACI can be considered an effective treatment option for symptomatic full-thickness cartilage defects. However, these results are presented in the absence of long-term patient-reported outcome measures, hence the need for longer follow-up studies.

In this work, our cell culture protocol allowed the generation of Cartibeads with hyaline-like features, namely a homogeneous distribution of safranin O–stained GAG, strong detection of type II collagen, and faint type I collagen staining. Quantitative detection of GAG showed that Cartibeads contained 24.6-μg/mg tissue (wet weight). While lower than native cartilage (≈60-μg/mg tissue, wet weight), this GAG content is higher than in previously reported studies and was expected, as Cartibeads are immature neocartilage tissues. Cartibeads showed a mean 35 ± 3–μg GAG/bead, which is 20-fold higher than previous studies, suggesting that our method produced more hyaline cartilage and less fibrocartilage.[2]

The use of adult chondrocytes as a source of cells to regenerate cartilage makes sense, as these cells should retain their original features. However, chondrocyte dedifferentiation usually occurs very rapidly in cell culture after passage 2, and redifferentiation is not possible from monolayer cell cultures beyond passage 3[20,30] unless using fetal or juvenile cartilage. This therefore requires a large amount of starting material, and in autologous protocols it implies high donor site morbidity. With our protocol, we have succeeded in completely standardizing the method of manufacturing Cartibeads regardless of patient age or quality of the starting cartilage biopsy specimen, using as little as 30 mg of harvest as compared with what is common (300 mg).[8]

Cartibeads are meant to treat focal chondral lesions by filling the defect completely after implantation and integrating with the surrounding tissue. After careful lesion debridement without inducing damage to the subchondral bone, Cartibeads are implanted, and the articular capsule is anatomically closed to re-create a favorable biological environment. Cartibeads then fuse to create homogeneous tissue. We hypothesize that cells on the surface and inside the Cartibeads have the ability to migrate and adhere to the subchondral bone and the native surrounding cartilage through their receptors on the cell surface. This is due to Cartibeads being a neocartilage tissue that is not yet mature, which preserves the cells' capacity to integrate within the lesion while secreting extracellular matrix with hyaline quality. At 3 months, full integration of the graft is observed in the lesions and, at 6 months, reorganization of the tissue in 3 layers as in the native cartilage.[35] The autologous implantation of Cartibeads in minipigs showed stable integration into lesions associated with a positive evolution of the graft toward cartilage tissue maturation, characterized by organization in 3 layers. This maturation and reorganization are shown between 3 and 6 months and supports the potential as a reliable solution with a stable native-like filling of the lesion and stabilization of the defect edges. Moreover, the implant maintained hyaline quality, as revealed by the intense detection of GAG and collagen II and the weak presence of collagens I and X, resulting in successful repair of cartilage damage at 6 months after implantation.

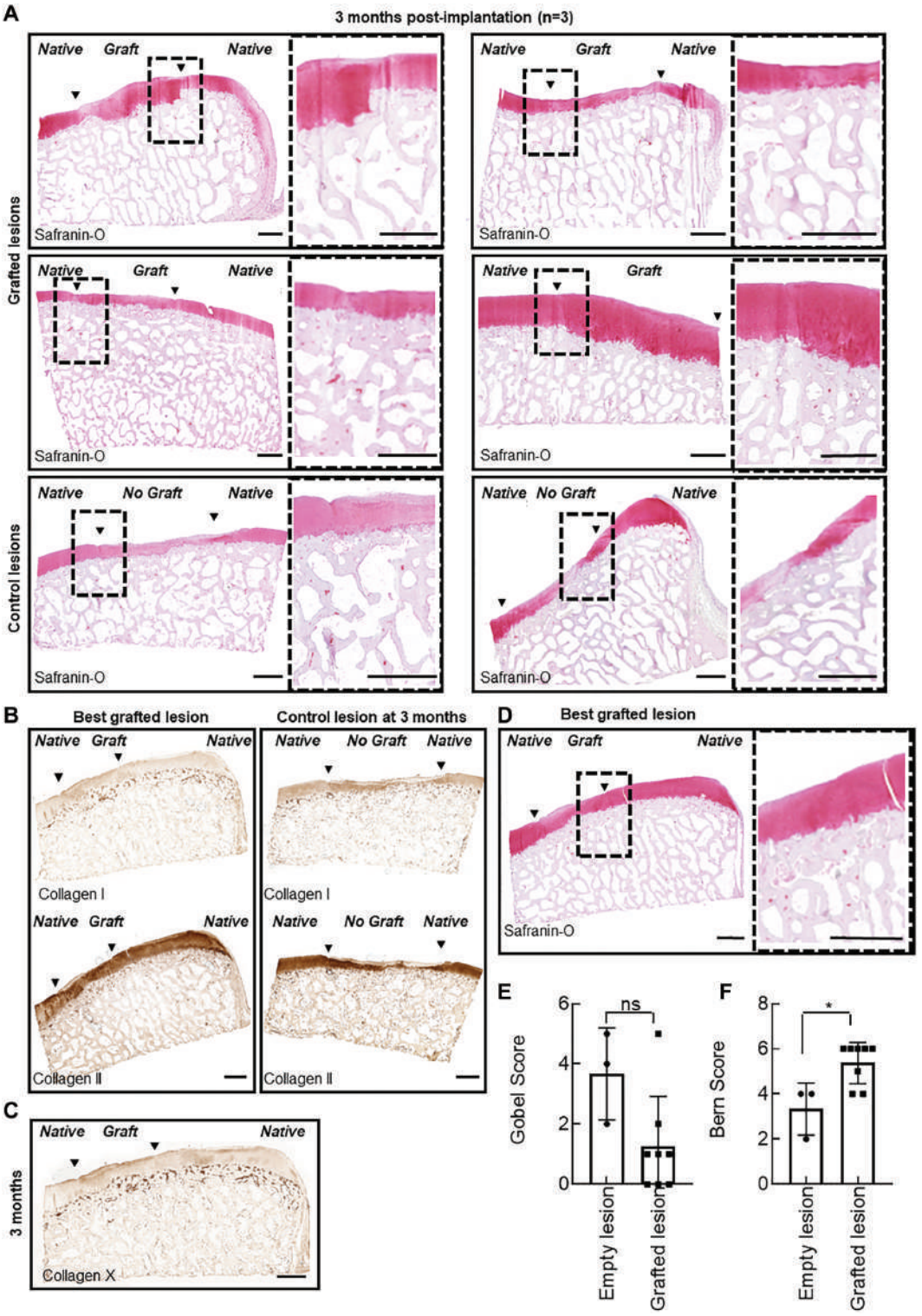

Figure 4. Integration of hyaline grafts in the knees of minipigs 3 months after implantation of autologous Cartibeads. (A) Safranin O staining of glycosaminoglycan of the 4 representative graft lesions (top panel) and 2 empty lesions as control (bottom panel) from the 3 minipigs. (B) Histological analysis of the best implanted lesion (left panel) and empty lesion (right panel) is shown, and the sections were stained for collagen I (top panels) and II (bottom panels). (C) Sections of the best implanted lesion stained for collagen X. (D) Safranin O staining of glycosaminoglycan of the best grafted lesion. (E) Histogram shows the Goebel score of the grafted and nongrafted lesions at 3 months. (F) Histogram shows the Bern score of the empty and grafted lesions at 3 months. Values are presented as mean ± SD. *$P < .05$. (A-D) The black arrowheads indicate the delimitation between native tissue and the graft. The enlarged segments show the tissue remodeling at 3 months postimplantation. Scale bar: 1000 μm.

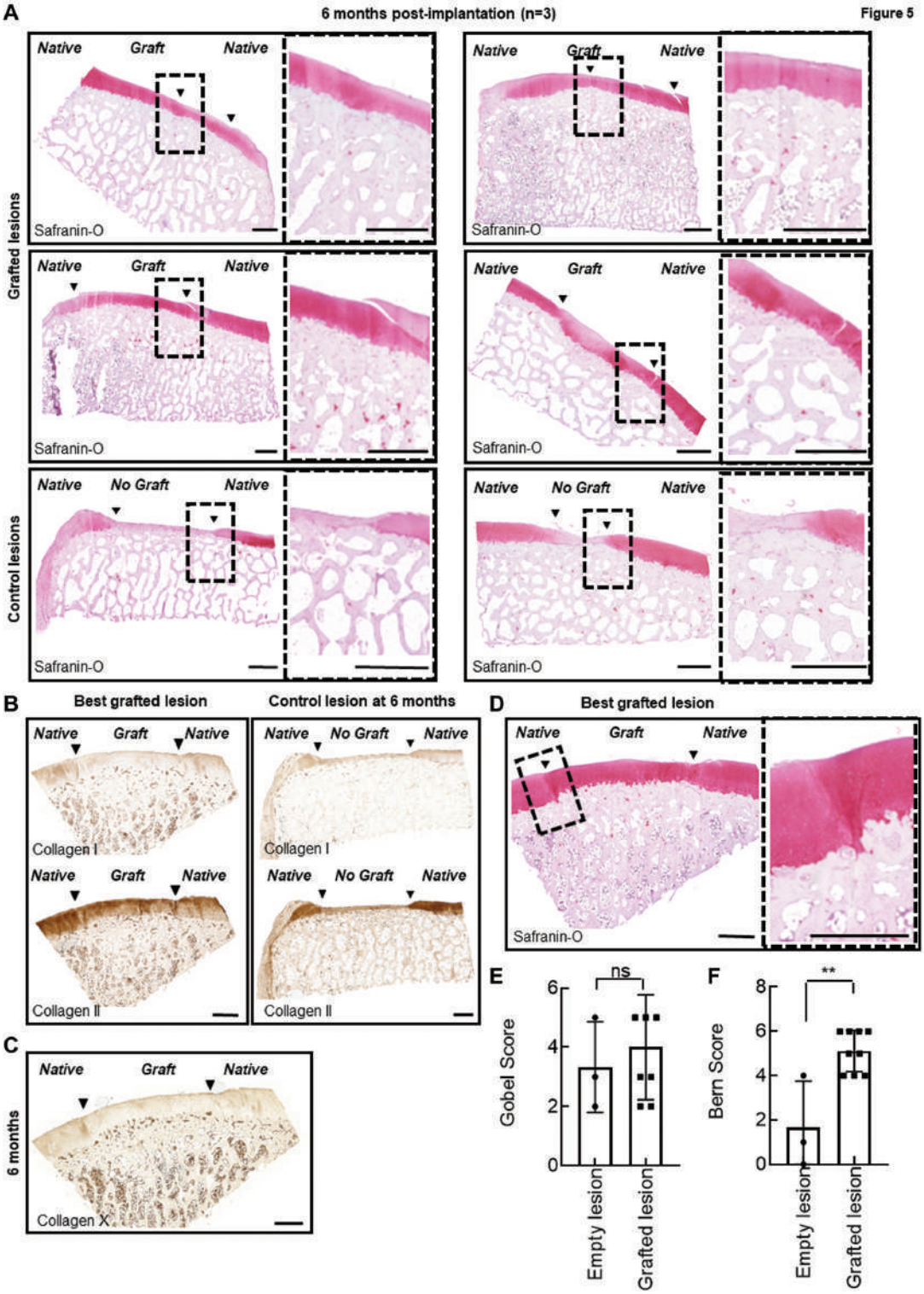

Figure 5. Integration of hyaline grafts in the knees of minipigs 6 months after implantation of autologous Cartibeads. (A) Safranin O staining of glycosaminoglycan of the 4 representative graft lesions (top panel) and 2 empty lesions as control (bottom panel) from the 3 minipigs. (B) Histological analysis of the best implanted lesion (left panel) and empty lesion (right panel) is shown, and the sections were stained for collagen I (top panels) and II (bottom panels). (C) Sections of the best implanted lesion stained for collagen X. (D) Safranin O staining of glycosaminoglycan of the best grafted lesion. (E) Histogram shows the Goebel score of the grafted and nongrafted lesions at 6 months. (F) Histogram shows the Bern score of the empty and grafted lesions at 6 months. Values are presented as mean ± SD. $^{**}P < .05$. (A through D) The black arrowheads indicate the delimitation between native tissue and the graft. The enlarged segments show the tissue remodeling at 3 months postimplantation. Scale bar: 1000 μm.

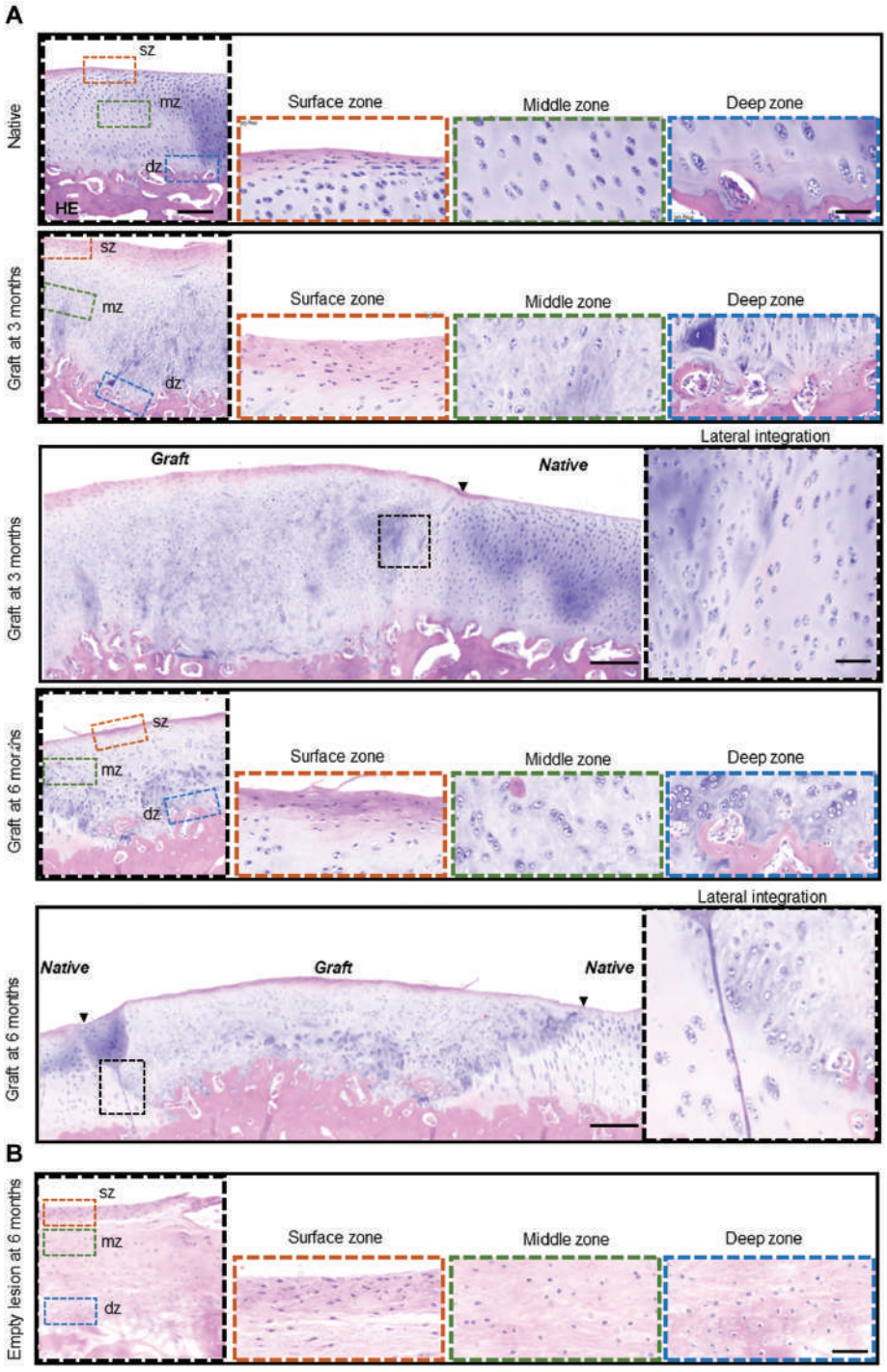

Figure 6. Histological analysis of the grafts and empty lesion at 3 and 6 months. (A) Hematoxylin and eosin (HE) staining of the native cartilage (upper panel). Scale bar: 500 μm. The grafts at 3 months (middle) and 6 months (bottom) with magnifications show the lateral integration. Scale bar: 500 μm and 200 μm in magnified cuts. sz, surface zone; mz, middle zone; dz, deep zone. Scale bar: 50 μm. Black arrowheads indicate the margins of the graft and native cartilage. (B) HE staining of the empty lesion at 6 months with magnifications showing the surface zone (sz), middle zone (mz), and deep zone (dz).

A significant improvement was observed in the histological scoring between lesions transplanted with Cartibeads and those left empty. Although we observed a trend toward improvement in the macroscopic Goebel Reverse Score,[15] we could not reach significance, most likely because of the modest sampling of the empty lesions. In addition,

lesions of 6 mm in diameter may not be sufficient to show a significant advantage of Cartibeads at the macroscopic level. These results are consistent with those of Ukai et al,[38] who demonstrated that distinguishing between fibrocartilage and hyaline cartilage is difficult when using only a macroscopic scoring system. Therefore, there is a need for assessing the composition of regenerative tissue by histological readout to meet the accurate definition of the tissue.[1,40]

The limitations of this study include the follow-up period, which was only up to 6 months without long-term results, and the sole use of empty lesions as a comparative, in addition to the published literature using similar therapies. Moreover, the animal sample size was small, and each animal presented multiple chondral defects, which might affect healing. This was not observed in this study since no degeneration of the joint was observed in animals at euthanasia.[7] The number of animals is similar to what is seen in other proof-of-concept studies.[29,32,42] Last, no functional assessment was performed on the repaired cartilage, but mechanical loading was assumed comparable to the native cartilage and contralateral knee since none of the animals showed limping, pathological gait, or pain on the grimace scale during the follow-up period. Another limitation of the study is that, ideally, we should have had only empty lesions in control minipigs. However, this was not allowed by our local ethics committee. To the best of our knowledge, the majority of implanted Cartibeads stayed in the intended lesion, but some may have detached and migrated to fill empty lesions. This was observed in our pilot study in domestic pigs, where most beads were seen in the lesions at 2 weeks after graft but some had detached. We hypothesize that this can occur because of the thin cartilage of the minipig knee (<1 mm) and the impossibility of immobilizing the animals after implantation of the Cartibeads.

The strength of the study is the use of multiple readouts with qualitative and quantitative analysis by different collaborating research and surgical teams.

CONCLUSION

We showed the feasibility of autologous Cartibeads implantation in a large animal model, supporting its potential for durable cartilage repair. Cartibeads are the first high-quality hyaline cartilage–engineered tissue from adult dedifferentiated chondrocytes used after extensive culture at high passage (up to passage 9) with integrative capacity to the native environment. The possibility of using high-passage chondrocytes makes it possible to bypass the use of stem cells with their associated risks (poor redifferentiation, tumor formation). Indeed, it is possible to obtain a large quantity of cells thanks to our technology (without the chondrocytes losing their original property of producing the hyaline matrix) and thus to treat large lesions. Collectively, the Cartibeads represent a breakthrough in the field of cartilage repair and have been approved by ethics committee and local medical authority for a first-in-human study using autologous cartilage implantation in patients with focal cartilage lesions.

ACKNOWLEDGMENT

The authors thank the technicians of the laboratory of Vincent Braunersreuther and Professor Karl-Heinz Krause for their help, as well as the team of Professor Walid Habre and the animal research facility of the University of Geneva. The authors also thank the personal of the genomic core facility of the Faculty of Medicine, University of Geneva, in particular Christelle Barracloug and Didier Chollet for their help in sample preparation, quantitative reverse transcription polymerase chain reaction, and RNA sequence, as well as Natacha Civic for RNA sequence analysis.

Authors

Halah Kutaish, MD, PhD (Department of Pathology and Immunology, Medical School, University of Geneva, Geneva, Switzerland. University Medical Center, University of Geneva, Geneva, Switzerland. Foot and Ankle Surgery Centre, Centre Assal, Clinique La Colline, Hirslanden Geneva, Switzerland); Philippe Matthias Tscholl, MD (Department of Orthopaedics Surgery, Geneva University Hospitals, Geneva, Switzerland); Erika Cosset, PhD (University Medical Center, University of Geneva, Geneva, Switzerland. Laboratory of Tumor Immunology, Oncology Department, Center for Translational Research in Onco-Hematology, Geneva University Hospitals, University of Geneva, Geneva, Switzerland); Laura Bengtsson, MSc (University Medical Center, University of Geneva, Geneva, Switzerland. Vanarix SA, Lausanne, Switzerland); Vincent Braunersreuther, PD, PhD (Service of Clinical Pathology, Diagnostic Department, Geneva University Hospitals, Geneva, Switzerland); Flavio Maurizio Mor, PhD (Tissue Engineering Laboratory, HEPIA/HES-SO, University of Applied Sciences and Arts Western Switzerland, Geneva, Switzerland); Jeremy Laedermann, PhD (Wyss Center for Bio and Neuroengineering, Geneva, Switzerland); Ivan Furfaro, PhD (Laboratory for Soft Bioelectronic Interfaces, Institute of Microengineering, Institute of Bioengineering, Centre for Neuroprosthetics, École Polytechnique Fédérale de Lausanne (EPFL), Switzerland); Dimitrios Stafylakis, MD (Department of Orthopaedics Surgery, Geneva University Hospitals, Geneva, Switzerland); Didier Hannouche, Prof., MD (University Medical Center, University of Geneva, Geneva, Switzerland. Department of Orthopaedics Surgery, Geneva University Hospitals, Geneva, Switzerland); Eric Gerstel, PD, MD (University Medical Center, University of Geneva, Geneva, Switzerland. Clinique la Colline, Hirslanden, Geneva, Switzerland); Karl-Heinz Krause, Prof., MD (Department of Pathology and Immunology, Medical School, University of Geneva, Geneva, Switzerland. University Medical Center, University of Geneva, Geneva, Switzerland); Mathieu Assal, PD, MD (University Medical Center, University of Geneva, Geneva, Switzerland. Foot and Ankle Surgery Centre, Centre Assal, Clinique La Colline, Hirslanden Geneva, Switzerland); Jacques Menetrey, Prof., MD (University Medical Center, University of Geneva, Geneva, Switzerland. Centre for Sports Medicine

and Exercise, Clinique la Colline, Hirslanden, Geneva, Switzerland); Vannary Tieng, PhD (University Medical Center, University of Geneva, Geneva, Switzerland. Vanarix SA, Lausanne, Switzerland)

REFERENCES

1. Abedian R, Willbold E, Becher C, Hurschler C. In vitro electromechanical characterization of human knee articular cartilage of different degeneration levels: a comparison with ICRS and Mankin scores. *J Biomech*. 2013;46(7):1328-1334.
2. Bartz C, Meixner M, Giesemann P, et al. An ex vivo human cartilage repair model to evaluate the potency of a cartilage cell transplant. *J Transl Med*. 2016;14(1):317.
3. Basad E, Ishaque B, Bachmann G, Sturz H, Steinmeyer J. Matrix-induced autologous chondrocyte implantation versus microfracture in the treatment of cartilage defects of the knee: a 2-year randomised study. *Knee Surg Sports Traumatol Arthrosc*. 2010;18(4):519-527.
4. Becher C, Laute V, Fickert S, et al. Safety of three different product doses in autologous chondrocyte implantation: results of a prospective, randomised, controlled trial. *J Orthop Surg Res*. 2017;12(1):71.
5. Benya PD, Padilla SR, Nimni ME. Independent regulation of collagen types by chondrocytes during the loss of differentiated function in culture. *Cell*. 1978;15(4):1313-1321.
6. Benya PD, Shaffer JD. Dedifferentiated chondrocytes reexpress the differentiated collagen phenotype when cultured in agarose gels. *Cell*. 1982;30(1):215-224.
7. Bonadio MB, Friedman JM, Sennett ML, et al. A retinaculum-sparing surgical approach preserves porcine stifle joint cartilage in an experimental animal model of cartilage repair. *J Exp Orthop*. 2017;4(1):11.
8. Brittberg M. Autologous chondrocyte implantation—technique and long-term follow-up. *Injury*. 2008;39(suppl 1):S40-S49.
9. Brittberg M, Lindahl A, Nilsson A, et al. Treatment of deep cartilage defects in the knee with autologous chondrocyte transplantation. *New Engl J Med*. 1994;331(14):889-895.
10. Brittberg M, Recker D, Ilgenfritz J, Saris DBF. Matrix-applied characterized autologous cultured chondrocytes versus microfracture: five-year follow-up of a prospective randomized trial. *Am J Sports Med*. 2018;46(6):1343-1351.
11. EMA. *CHMP Assessment Report: Spherox*. EMA; 2017.
12. Eschen C, Kaps C, Widuchowski W, et al. Clinical outcome is significantly better with spheroid-based autologous chondrocyte implantation manufactured with more stringent cell culture criteria. *Osteoarthritis Cartilage Open*. 2020;2(1):100033.
13. Falah M, Nierenberg G, Soudry M, Hayden M, Volpin G. Treatment of articular cartilage lesions of the knee. *Int Orthop*. 2010;34(5):621-630.
14. Gobbi A, Karnatzikos G, Kumar A. Long-term results after microfracture treatment for full-thickness knee chondral lesions in athletes. *Knee Surg Sports Traumatol Arthrosc*. 2014;22(9):1986-1996.
15. Goebel L, Orth P, Müller A, et al. Experimental scoring systems for macroscopic articular cartilage repair correlate with the MOCART score assessed by a high-field MRI at 9.4 T—comparative evaluation of five macroscopic scoring systems in a large animal cartilage defect model. *Osteoarthritis Cartilage*. 2012;20(9):1046-1055.
16. Gotterbarm T, Breusch SJ, Schneider U, Jung M. The minipig model for experimental chondral and osteochondral defect repair in tissue engineering: Retrospective analysis of 180 defects. *Lab Anim*. 2008;42(1):71-82.
17. Grogan SP, Barbero A, Winkelmann V, et al. Visual histological grading system for the evaluation of in vitro-generated neocartilage. *Tissue Eng*. 2006;12(8):2141-2149.
18. Grossman AD, Den Haese JP Jr, Georger L, McMillan S, Tuck JA. Matrix-induced autologous chondrocyte implantation (MACI) is largely effective and provides significant improvement in patients with symptomatic, large chondral defects: a systematic review and meta-analysis. *Surg Technol Int*. 2022;41:sti41/1613. doi:10.52198/22.STI.41.OS1613
19. Hettrich CM, Crawford D, Rodeo SA. Cartilage repair: third-generation cell-based technologies—basic science, surgical techniques, clinical outcomes. *Sports Med Arthrosc Rev*. 2008;16(4):230-235.
20. Huang BJ, Hu JC, Athanasiou KA. Cell-based tissue engineering strategies used in the clinical repair of articular cartilage. *Biomaterials*. 2016;98:1-22.
21. Kessler MW, Ackerman G, Dines JS, Grande D. Emerging technologies and fourth generation issues in cartilage repair. *Sports Med Arthrosc Rev*. 2008;16(4):246-254.
22. Kon E, Gobbi A, Filardo G, et al. Arthroscopic second-generation autologous chondrocyte implantation compared with microfracture for chondral lesions of the knee: prospective nonrandomized study at 5 years. *Am J Sports Med*. 2009;37(1):33-41.
23. Kreuz PC, Steinwachs MR, Erggelet C, et al. Results after microfracture of full-thickness chondral defects in different compartments in the knee. *Osteoarthritis Cartilage*. 2006;14(11):1119-1125.
24. Lee JK, Huwe LW, Paschos N, et al. Tension stimulation drives tissue formation in scaffold-free systems. *Nat Mater*. 2017;16(8):864-873.
25. Madeira C, Santhagunam A, Salgueiro JB, Cabral JM. Advanced cell therapies for articular cartilage regeneration. *Trends Biotechnol*. 2015;33(1):35-42.
26. McAdams TR, Mithoefer K, Scopp JM, Mandelbaum BR. Articular cartilage injury in athletes. *Cartilage*. 2010;1(3):165-179.
27. Mithoefer K, McAdams T, Williams RJ, Kreuz PC, Mandelbaum BR. Clinical efficacy of the microfracture technique for articular cartilage repair in the knee: an evidence-based systematic analysis. *Am J Sports Med*. 2009;37(10):2053-2063.
28. Mumme M, Barbero A, Miot S, et al. Nasal chondrocyte-based engineered autologous cartilage tissue for repair of articular cartilage defects: an observational first-in-human trial. *Lancet*. 2016;388(10055):1985-1994.
29. Mumme M, Steinitz A, Nuss KM, et al. Regenerative potential of tissue-engineered nasal chondrocytes in goat articular cartilage defects. *Tissue Eng Part A*. 2016;22(21-22):1286-1295.
30. Munirah S, Samsudin OC, Aminuddin BS, Ruszymah BH. Expansion of human articular chondrocytes and formation of tissue-engineered cartilage: a step towards exploring a potential use of matrix-induced cell therapy. *Tissue Cell*. 2010;42(5):282-292.
31. Negoro T, Takagaki Y, Okura H, Matsuyama A. Trends in clinical trials for articular cartilage repair by cell therapy. *NPJ Regen Med*. 2018;3:17.
32. Nettles DL, Kitaoka K, Hanson NA, et al. In situ crosslinking elastin-like polypeptide gels for application to articular cartilage repair in a goat osteochondral defect model. *Tissue Eng Part A*. 2008;14(7):1133-1140.
33. Niemeyer P, Laute V, Zinser W, et al. A prospective, randomized, open-label, multicenter, phase III noninferiority trial to compare the clinical efficacy of matrix-associated autologous chondrocyte implantation with spheroid technology versus arthroscopic microfracture for cartilage defects of the knee. *Orthop J Sports Med*. 2019;7(7):2325967119854442.
34. Pathak S, Chaudhary D, Reddy KR, Acharya KKV, Desai SM. Efficacy and safety of CARTIGROW in patients with articular cartilage defects of the knee joint: a four year prospective studys. *Int Orthop*. 2022;46(6):1313-1321.
35. Pauli C, Whiteside R, Heras FL, et al. Comparison of cartilage histopathology assessment systems on human knee joints at all stages of osteoarthritis development. *Osteoarthritis Cartilage*. 2012;20(6):476-485.
36. Ramezankhani R, Torabi S, Minaei N, et al. Two decades of global progress in authorized advanced therapy medicinal products: an emerging revolution in therapeutic strategies. *Front Cell Dev Biol*. 2020;8:547653.
37. Saris D, Price A, Widuchowski W, et al. Matrix-applied characterized autologous cultured chondrocytes versus microfracture: two-year follow-up of a prospective randomized trial. *Am J Sports Med*. 2014;42(6):1384-1394.

38. Ukai T, Sato M, Wasai S, et al. Comparison of properties determined using electromechanical assessment (Arthro-BST) with macroscopic and histological properties in symptomatic human articular cartilage of the hip. *Arthritis Res Ther*. 2021;23(1):227.
39. Vonk LA, de Windt TS, Slaper-Cortenbach IC, Saris DB. Autologous, allogeneic, induced pluripotent stem cell or a combination stem cell therapy? Where are we headed in cartilage repair and why: a concise review. *Stem Cell Res Ther*. 2015;6:94.
40. Widhiyanto L, Utomo DN, Perbowo AP, Hernugrahanto KD. Macroscopic and histologic evaluation of cartilage regeneration treated using xenogenic biodegradable porous sponge cartilage scaffold composite supplemented with allogenic adipose derived mesenchymal stem cells (ASCs) and secretome: an in vivo experimental study. *J Biomater Appl*. 2020;35(3):422-429.
41. Wu L, Gonzalez S, Shah S, et al. Extracellular matrix domain formation as an indicator of chondrocyte dedifferentiation and hypertrophy. *Tissue Eng Part C Methods*. 2014;20(2):160-168.
42. Zhang Y, Liu S, Guo W, et al. Human umbilical cord Wharton's jelly mesenchymal stem cells combined with an acellular cartilage extracellular matrix scaffold improve cartilage repair compared with microfracture in a caprine model. *Osteoarthritis Cartilage*. 2018;26(7):954-965.